JOM
The Journal of The Minerals Metals & Materials Society

The Intelligent Control of an Inert-Gas Atomization Process

S.A. Osella, S.D. Ridder, F.S. Biancaniello and P.I. Espina

Reprinted from JOM, Vol. 43, No. 1, January, 1991, p. 18-21

The Intelligent Control of an Inert-Gas Atomization Process

S.A. Osella, S.D. Ridder, F.S. Biancaniello and P.I. Espina

Intelligent control is an attempt to specify the function of a controller in ways which mimic the decision-making capabilities of humans. Traditionally, issues relating to the emulation of human-like capabilities have fallen in the domain of artificial intelligence. Intelligent processing is a specific form of intelligent control in which the system to be controlled is a process rather than the more conventional mechanical or electrical system. The National Institute of Standards and Technology's program on intelligent processing of metal powders is a multi-disciplinary research initiative investigating the application of intelligent control technologies to improve the state of the art of metal powder manufacturing. This paper reviews the design of the institute's supersonic inert-gas metal-atomizer control system.

INTRODUCTION

In broad terms, intelligence has been defined as that which improves an organism's ability to produce successful behavior.[1] Successful behavior depends on the objective of the organism, the physical capabilities of the organism, and the environment within which the organism is acting.

Research into intelligence has been closely associated with research into the control of movement. This can be understood by considering that the only overt manifestation of intelligence is movement. From this perspective, it has been argued that the brain is first and foremost a control system.[2] Animals are equipped with nervous systems which, through a succession of nerve cell layers, analyze sensory inputs of different modalities to achieve an understanding of the world around them. Outgoing nerve signals from the motor cortex are compared with the incoming (feedback) sensory signals to produce accurate and coordinated behavior.

Issues relating to the emulation of intelligent behavior have traditionally fallen under the domain of artificial intelligence (AI). It is interesting to note, however, that Cybernetics, a movement in the 1930s headed by Norbert Weiner, a control theorist, was the first concerted effort to construct an intelligent machine. Having begun with the common goal of designing machines capable of satisfactory performance in uncertain conditions, control theorists and AI researchers today have diverged into interests with seemingly disparate goals. Recently, the desire for greater versatility has reunited the two fields in an attempt to achieve robust "intelligent" control and behavior.

Intelligent control is an attempt to specify the function of a controller in ways which mimic the decision-making capabilities of humans. Although the term was first put into common practice by Saridis,[3] the concept encompasses far more than can be attributed to one individual. Essentially, knowledge about the system to be controlled (e.g., a manufacturing plant) is typically encoded using production rules, frames and/or object-oriented data structures. Control of the plant is carried out through goal-driven and/or data-driven strategies. By design, the control system representation is heuristic; therefore, it is, in general, greatly approximative.

Intelligent processing is a specific form of intelligent control by which the system to be controlled is a process rather than the more conventional mechanical or electrical system. This complicates matters because the differential equations which govern the behavior of the process are more difficult to determine. One approach to this problem is to use computational models.

The National Institute of Standards and Technology's (NIST's) program on intelligent processing of materials is a broad-based research initiative investigating the application of intelligent control to improve the state of the art in material processing. In particular, NIST is researching the processing of metal powders using close-coupled supersonic inert-gas atomization.

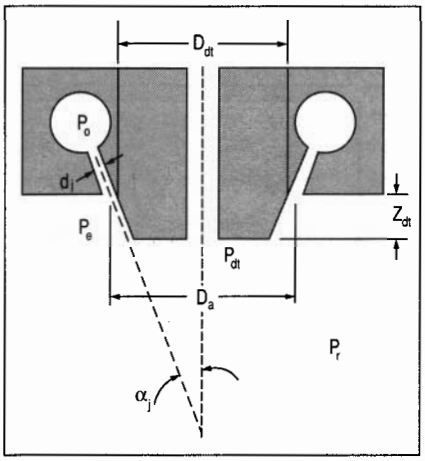

Figure 1. A schematic cross-section of the atomization assembly.

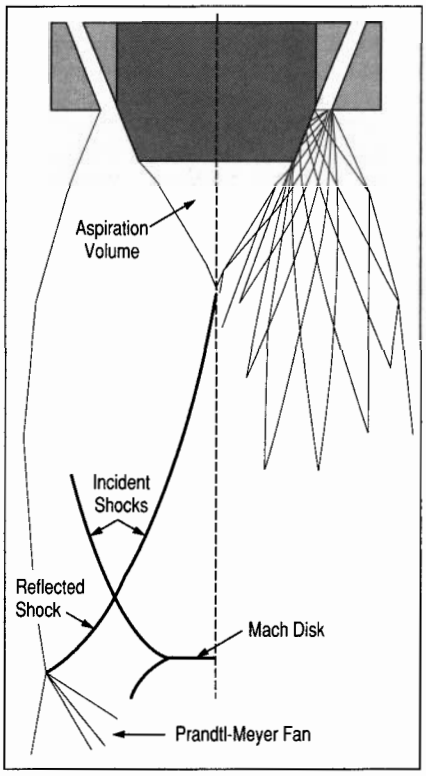

Figure 2. Gas flow analysis by method of characteristics with schematic representation of shock formation (P_o = 7.0 MPa, P_o/P_r = 71).

SUPERSONIC INERT-GAS METAL ATOMIZATION

Several important properties of metal powder (and their consolidated products) are dependent on as-atomized particle size.[4,5] These properties include mechanical performance (e.g., strength, toughness, creep resistance, etc.) as well as physical characteristics of the powder itself (e.g., particle shape, porosity, flow qualities, etc.). Most of these properties improve as particle size decreases; however, powder handling becomes more complicated for finer powder because of caking, environmental contamination, pyrophoricity and other effects. The strong dependence of properties on particle size translates into an increased demand on the process engineer to dynamically control this aspect of the atomization process.

Efficient control of a process requires a detailed understanding of how the

product is formed. In a gas metal atomizer, the powder product solidifies from liquid droplets generated by the interaction of energetic gas jets with a supply of molten metal. NIST's supersonic inert-gas metal atomizer (SIGMA) has been found to be particularly efficient in producing fine powders (50% by weight less than 30 μm) for a wide range of alloys.[6] The primary design differences distinguishing the system from most conventional gas atomizers are the arrangement of gas jets relative to the molten metal stream and the high-pressure gas delivery system used to achieve supersonic gas jet velocities.

The atomizing nozzle assembly or die, shown schematically in Figure 1, is composed of 18 gas nozzles arranged concentric to the liquid delivery tube with an inter-jet diameter (D_a) of 11.5 mm. Each individual jet has a diameter (d_j) of 0.8 mm. The jets are aimed at an angle (α_j) of 22.5 degrees with respect to the axis of symmetry of the delivery tube. The delivery tube extends out of the jet exit plane a distance (Z_{dt}) equal to 2.54 mm, with a diameter (D_{dt}) equal to 9.91 mm. Also indicated in Figure 1 are locations used to measure several pressure values. These include the plenum or gas jet stagnation pressure (P_o), the gas jet exit pressure (the pressure to which a gas expands in reaching sonic velocity, P_e), the liquid delivery tube or aspiration pressure (P_{dt}), and the exit reservoir pressure (P_r), which is 100 kPa.

The resultant powder size is directly related to the die geometry and process parameters. Consequently, the gas-metal interaction was studied to provide the necessary process understanding to develop control strategies.

PROCESS ANALYSIS AND MODELING

The first and necessary step in the design of a control system is to determine plant dynamics. With mechanical and electrical systems, the characteristics can be determined either by measuring the response of the system or by mathematical modeling using well-established component characteristics. Similar methodologies can be employed when the system to be controlled is a process. In modeling a process, however, one generally has to begin at a low level and build up to the system level. This approach requires assumptions to be postulated which can only be verified after the behavior of the composite system is observed.

Several flow visualization techniques (i.e., schlieren, 25 ns pulsed-laser holography and 20,000 frames-per-second cinematography) were used to study gas only and gas-liquid atomization flow fields produced by the SIGMA system. Figure 2 shows the results of a two-dimensional gas flow analysis using the

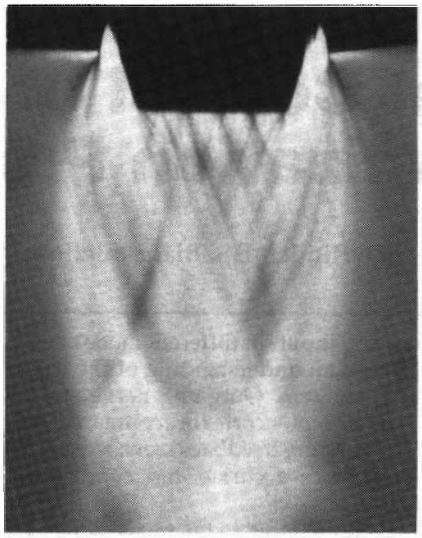

Figure 3. Schlieren photo of gas flow (P_o = 7.0 MPa, P_o/P_r = 71).

method of characteristics for P_o = 7.0 MPa, along with a schematic representation of the curved shock formation as discussed below and seen in the schlieren photograph in Figure 3. A detailed discussion of compressible jet theory can be found in Reference 7.

The diamond-shaped areas on the right half of Figure 2 represent regions of constant flow properties bounded by characteristic waves. The calculation of characteristic waves began at the nozzle exit and proceeded downstream until the first shock wave was encountered. At this point the calculation was stopped because Prandtl-Meyer theory only pertains to isentropic, irrotational flow and does not support the existence of shock waves.[7]

Referring to Figure 2, at the exit of the nozzle, the flow undergoes an expansion fan in decreasing its pressure from P_e to P_r. Although the number of fans that originate at the corner is infinite, a discrete number was selected to allow a solution by the method of characteristics. Flow properties were calculated in each sector bounded by characteristic lines proceeding to the last sector in the fan, where the free boundary condition is satisfied ($P = P_r$).[8]

The calculated free-jet (constant pressure) boundary and shock waves agree very well with the schlieren photo in Figure 3, where the free boundary is clearly visible and the shocks are seen as crossing lines near the geometric convergence point of the jets. The contrast in the schlieren photograph primarily results from the gas density gradients integrated over the length of the light path. Integration of the gas density gradient results in the superposition of information from the full volume of the jet passed by the light rays. This is more apparent in the upper regions of the picture just below the edge of the delivery tube where individual jets from each side of the die combine to produce the complex patterns seen in this region.

Aspiration pressure measurements were made on the atomizing die in the absence of liquid flow. Pressures were measured in the gas plenum (P_o) and at the exit of the liquid delivery tube (P_{dt}), as depicted in Figure 1. Aspiration measurements were taken using three gases (nitrogen, argon and helium) while varying P_o from 363 kPa to 11.2 MPa (the P_o/P_r ratio varied from 3.63 to 112). The results of the aspiration pressure measurements for the three gases are shown in Figure 4. Although the details for each curve (location of slope changes, minimums and maximums) are different, the overall shapes are quite similar. The features of interest seen in each curve are the maximums of P_{dt}/P_r for values of $P_o/P_r < 20$, the plateaus in each curve for $30 < P_o/P_r < 60$, the minimums in P_{dt}/P_r, and the gradual rise in P_{dt}/P_r as P_o/P_r increases past the point where the minimum occurs.

The results of the characteristic analysis indicate a peak Mach number value of 8.73 and a minimum pressure value of 0.06 P_r (6.0 kPa) in the jet. These calculations show that aspiration is the result of free expansion within the supersonic jets, which overshoots the free jet boundary value (P_r) and continues expanding to pressures below P_r. Figure 5 shows a generalized aspiration curve that reproduces the important features of the curves shown in Figure 4. Also shown in this figure is a simplified characteristic analysis for an underexpanded jet with

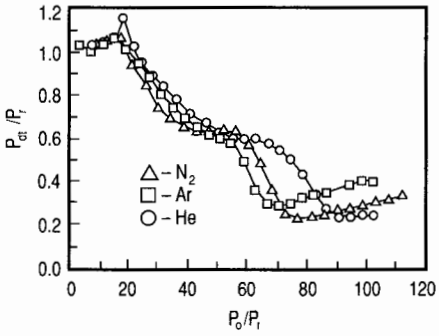

Figure 4. Aspiration curves for nitrogen, argon and helium.

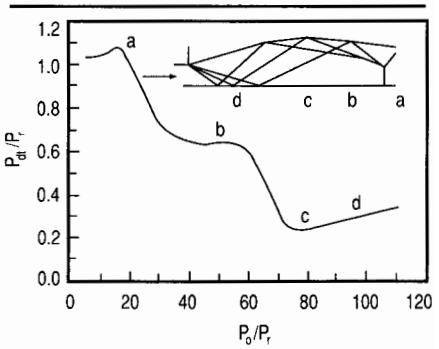

Figure 5. Generalized aspiration curve showing the predominant features of the curves shown in Figure 4.

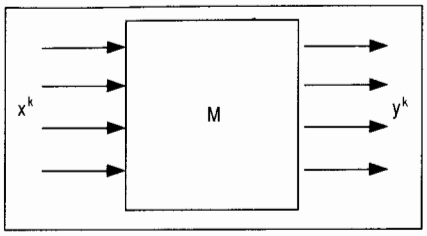

Figure 6. Block diagram of a pattern recognition system.

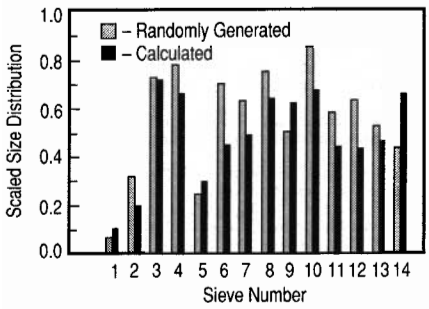

Figure 7. Comparison of a randomly generated particle size distribution with that calculated by the neural network.

positions along the boundary marked to represent the location of the delivery tube corner (the aspirating location) for various pressure ratios. The condition marked "a" corresponds to the peak in aspiration and results from operating the nozzles at low pressure ratios that place the shock wave near the delivery tube corner. Condition "b" is reached as the pressure ratio increases and the region of compression preceding the shock moves to the aspirating location. Condition "c," corresponding to the aspiration minimum, occurs when the region of maximum expansion is moved to this position, and, finally, condition "d" is reached for any further increase in the pressure ratio.

NONDESTRUCTIVE EVALUATION OF PRODUCT QUALITY

Traditional process control typically involves statically defining process parameter set-points, processing the product, evaluating the product and changing the process parameters to improve process output. It is the aim of process feedback control to use process output information, acquired during production, to guide the on-line adjustment of process parameters to beneficially affect the process output.

The size of the metal powder particles produced by the SIGMA is determined on-line by passing a laser beam through the particle flow, measuring the intensity distribution of the light scattered by the particles and using the relationship between the particle size and light intensity distributions. The light scattering (Fraunhofer diffraction) phenomena can be described by the following equation:

$$e = Tw \qquad (1)$$

where w is the particle size distribution discretized into a number of bins of prescribed particle diameter ranges, e is the light intensity distribution incident on detector diodes of specified radial thicknesses, and T is the model of the Fraunhofer diffraction in matrix form.[9] The accuracy of this mathematical model has been demonstrated by comparisons with measured light intensity distributions produced by a stationary particle size distribution.[10]

The ability to describe the optics using a matrix, as in Equation 1, suggests the calculation of the particle size distribution using the inverse of the T matrix such that

$$w = T^{-1}e \qquad (2)$$

Although calculating the inverse of a matrix is mechanically a trivial matter, the matrix to be inverted must possess certain properties so that when inverted, the solution produces physically realizable particle size distributions. Due to the nature of the scattering effect and, thus, composition of the transformation matrix T, calculation of particle size distributions by way of Equation 2 has proven to be, as yet, infeasible.

The approach taken to solve the inverse transformation problem involved the use of an adaptive pattern recognition algorithm. As illustrated in Figure 6, the signals x^k in R^n space input to a pattern recognition system are transformed into the output signals y^k in R^m space by a transfer function (also called associative mapping) of the form:

$$y^k = M(x^k) \qquad (3)$$

The problem of pattern recognition, called the paired-associate problem, is to derive a function M such that for every pair $\{(x^k, y^k), k = 1, 2, \ldots, p\}$, Equation 3 is satisfied.[11] The calculation of a particle size distribution from a light intensity distribution can be formulated as a paired-associate problem, where the pattern x^k input to the pattern recognition system is a measured light intensity distribution vector:

$$e^k = \{e^{k_1}, e^{k_2}, \ldots, e^{k_n}\}$$

and the output y^k is the corresponding particle size distribution vector:

$$w^k = \{w^{k_1}, w^{k_2}, \ldots, w^{k_m}\}$$

for $k = 1, 2, \ldots, p$.

The associative mapping which performs the inverse transformation was generated using an adaptive pattern recognition algorithm based on the principle of neural computing. Figure 7 depicts the comparison of a randomly generated particle size distribution, simulating the passing of metal particles through the sensor's measurement volume, with that calculated by the pattern recognition system. Although there is strong correlation between the two histograms, there are a few sieve bins with considerable discrepancies.

This level of performance is considered quite high for real-time particle size analysis. Because Fraunhofer diffraction is a nonlinear transformation, small differences in the light intensity distributions greatly magnify the differences in the particle size distributions. Figure 8, which illustrates the light intensity distributions corresponding to the particle size distributions of Figure 7, demonstrates this phenomenon. As can be seen, the light intensity distributions are virtually indistinguishable.

EXPERT CONTROL OF THE ATOMIZATION PROCESS

Figure 9 diagrams the architecture of the SIGMA's process control system. The high-level controller refers to a physically remote computer with which an operator can interact via the keyboard and graphics monitor. The world model is a database describing the state of the

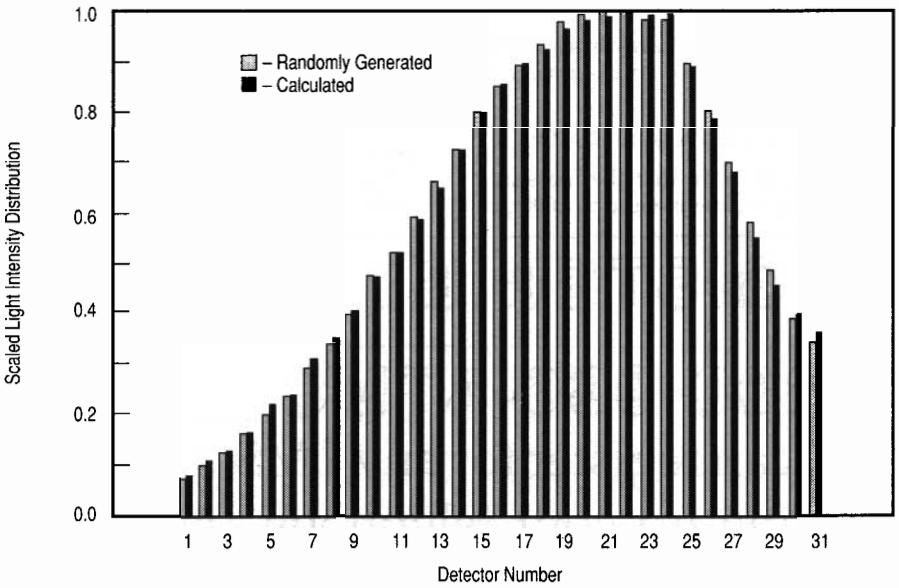

Figure 8. Light intensity distributions corresponding to the particle size distributions of Figure 7.

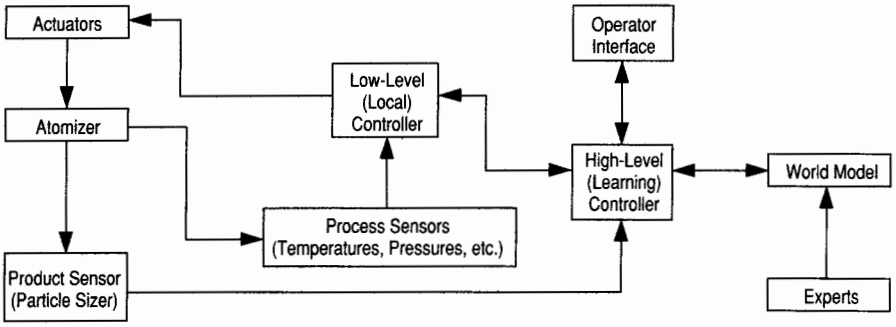

Figure 9. A schematic diagram of the atomizer control system.

atomization process, which is continuously updated during processing. The low-level controller performs the direct data acquisition and actuation as well the time-critical control functions. The product sensor is the previously described in-situ particle sizer.

The high-level controller's decision-making strategy is based on the principle of hierarchical control.[12] In this approach, the strategy is considered to be goal-directed. The controller's highest level goal, the objective, is decomposed into a number of more elementary sub-goals. All of the sub-goals have to be achieved to accomplish the objective.

To carry out the necessary goal decomposition, the controller is divided into a number of control modules. The control modules are related in such a way that a next lower level module is responsible for the accomplishment of one or more of the sub-goals. Each sub-goal becomes the objective for that lower level module, resulting in a recursive definition of the overall objective.

The knowledge required to decompose a module's objective is called the control knowledge and is stored in its knowledge-base in the form of facts and production rules. A fact in the knowledge-base has the following form:

[*relation* item-1 (item-2 ... item-N)]

The items in the fact are associated by the given relationship. An example of an asserted fact is

(*equal-to* Die-Pressure 1000.00)

which could mean that the measured pressure in the die plenum is 1,000 psi. The exact meaning of a fact depends on its use in a production rule.

A production rule specifies the action that is to take place when a given condition is encountered. As a result, a rule has the following form:

IF condition THEN action.

The condition, also called stimulus or state, is made up of a number of facts. When all of the facts which make up a rule's condition have been asserted (entered in the knowledge-base), the rule is said to be triggered. More than one rule can be triggered simultaneously. A conflict-resolution policy is used to select from among the triggered rules. When a rule is selected, it is said to be fired. When a rule is fired, the rule's action, also called a response, is performed.

If only one rule can be triggered at any one time, the rules in the knowledge-base make up what is called a state-table. If the policy used to select a rule is variable, the controller is considered to be adaptive. If the manner in which the selection policy is varied leads to a better performance, the controller is said to be learning. All of the these methods make up the intelligent decision making of the atomizer's control system.

As currently designed, most of the SIGMA's control knowledge is of the pre-programmed type, which is acquired from an understanding (albeit incomplete) of the atomization process. The software is designed to permit easy development and modification of the control knowledge and architecture used to execute atomization runs. As new knowledge is acquired, it can quickly be added to the knowledge-base. Similarly, as new sensors or actuators are added to the atomizer system, additional control modules can be incorporated in the controller.

References

1. J.S. Albus, "A Theory of Intelligent Systems," paper presented at the Fifth IEEE International Symposium on Intelligent Control, Philadelphia, PA (Sept. 5–7, 1990).
2. J.S. Albus, "Mechanisms for Planning and Problem Solving in the Brain," *Mathematical Biosciences*, 45 (1979), pp. 247–293.
3. G.N. Saridis, "Foundations of the Theory of Intelligent Controls," *Proceedings IEEE Workshop on Intelligent Control* (1985).
4. W.J. Boettinger, L. Bendersky and J.G. Early, "An Analysis of the Microstructure of Rapidly Solidified Al-8 Wt Pct Fe Powder," *Met. Trans. A*, 17 (1986), pp. 781–790.
5. S.D. Ridder and F.S. Biancaniello, "Process Control During High Pressure Atomization," *Mat. Sci. Eng.*, 98 (1988), pp. 47–51.
6. F.S. Biancaniello et al., "Particle Size Measurement of Inert-Gas-Atomized Powder," *Mat. Sci. Eng.*, A124 (1990), pp. 9–14.
7. A.H. Shapiro, *The Dynamics and Thermodynamics of Compressible Fluid Flow* (New York: John Wiley & Sons, 1953).
8. P.I. Espina et al., "Aerodynamic Analysis of the Aspiration Phenomena in a Close-Coupled Inert Gas Atomizer," *Characterization & Diagnostics of Ceramics & Metal Particulate Processing* (Warrendale, PA: TMS, 1989), pp. 49–62.
9. J. Swithenbank et al., "A Laser Diagnostic Technique for the Measurement of Droplet and Particle Size Distribution," Paper presented at the AIAA 14th Aerospace Sciences Meeting (January 1976).
10. E.D. Hirleman and G. Dodge, "Performance Comparisons Malvern Instruments Laser Diffraction Drop Size Analyzers," *International Conference of Liquid Atomization and Spray Systems (ICLASS-85)* (London: Institute of Energy, 1985).
11. T. Kohonen, *Self-Organization and Associative Memory*, 2nd ed. (New York: Springer-Verlag, 1988).
12. J.S. Albus, H.G. McCain and R. Lumia, "NASA/NBS Standard Reference Model for Tellerobot Control System Architecture (NASREM)," *NIST Technical Note 1235*, 1989.

ABOUT THE AUTHORS

S.A. Osella received his M.S. in mechanical engineering from George Washington University in 1986. He is currently a research scientist at the National Institute of Standards and Technology (NIST).

S.D. Ridder received his Ph.D. in metallurgy from the University of Illinois in 1980. He is currently a metallurgist at NIST. Dr. Ridder is also a member of TMS.

F.S. Biancaniello received his B.S. in industrial technology from the University of Maryland in 1977. He is currently a metallurgist at NIST. Mr. Biancaniello is also a member of TMS.

P.I. Espina received his B.S. in mechanical engineering from the University of Puerto Rico in 1987. He is currently a research scientist at NIST.

If you want more information on this subject, please circle reader service card number 52.